MEASUREMENT UNCERTAINTY OF COMPLEX-VALUED MICROWAVE QUANTITIES

Yu Song Meng* and Yueyan Shan

National Metrology Centre, Agency for Science, Technology and Research (A*STAR), 1 Science Park Drive, Singapore 118221, Singapore

Abstract—This paper presents an evaluation of measurement uncertainty for complex-valued quantities in microwave applications, mainly focusing on the non-linear transformation of measurement uncertainty from rectangular coordinate to polar coordinate. Based on the *law of propagation of uncertainty* in matrix form, general expressions of the covariance matrix for the magnitude and phase uncertainties in polar coordinate have been derived, and several different application scenarios have been analyzed and evaluated with numerical simulations. This is followed by some recommendations on the coordinate transformations in practical microwave measurements.

1. INTRODUCTION

Measurements of complex-valued quantities are often experienced in microwave applications, such as Scattering parameter (S-parameter) and equivalent source reflection coefficient [1–4]. Analysis and evaluation of the uncertainty in a measurement is very important as it can itemize those known sources of errors and also quantify their combined influence on the best estimates [5–9]. In Singapore, National Metrology Centre (NMC) of the Agency for Science, Technology and Research (A*STAR) serves as the custodian of the national standards. We are responsible for the establishment, maintenance and dissemination of the microwave related national standards and also provide the necessary calibration services to the industry. This requires us to analyze and evaluate the measurement uncertainty properly.

For the often experienced complex-valued microwave quantities, the associated measurement uncertainties have been strongly recommended to be evaluated in rectangular coordinate [10], following the internationally recommended guidelines [5]. More efforts on the evaluations of measurement uncertainty for complex-valued quantities can be found in [11–14]. From these studies, it is found that when using sample statistics to evaluate the uncertainty of a complex-valued quantity, polar coordinate is suggested to be avoided. However, the magnitude and phase representations in polar coordinate are sometimes preferred and more "natural" [13] for many microwave component measurements like amplifier, attenuator, coupler. This is because the representation in polar coordinate bears a direct relationship to some physical phenomena affecting the measurement process. For example in microwave applications, phase is directly related to the electrical path length of a signal, while magnitude is directly related to the amplified/attenuated level of a transmitted signal [10]. Therefore, it is often required to evaluate the measurement uncertainties of the magnitude and phase representations in polar coordinate.

From the literature, transformation of the uncertainty evaluated in rectangular coordinate to polar coordinate is suggested to be a good solution [10]. However the transformation has not yet been fully explored for realistic measurement scenarios. The transformation is non-linear and is not always reliable for the practical implementations [11]. In most of works [10–14], covariance matrix which groups together information about the standard uncertainties and correlation between the real and imaginary components has been used to describe the complex-valued quantities. With the covariance matrix, the uncertainty evaluated in the rectangular coordinate could be transformed into the desired polar coordinate using the *law of propagation of uncertainty* in matrix form [10, 13, 14].

We have carried out some preliminary works in [3] for the non-linear coordinate transformation based on the measurement data with relatively small size (6 samples following our internal calibration procedure for industry). It is noted that the estimated correlation coefficient in covariance matrix is rarely meaningful based on such relatively small sample sizes (other examples are 5 to 6 samples in [1, 10]), and is inherently unreliable for practical measurements. Hence, the proposed method in [3] has limited applications without detailed knowledge of its dependence on the correlation coefficient in the covariance matrix.

Therefore, in this paper we further investigate the uncertainty propagation/transformation from rectangular coordinate to polar coordinate. The influence from the correlation between the real and

imaginary components is studied. Numerical simulations with pre-assigned properties are carried out, and geometric representations of the simulated complex-valued quantities are used for understanding the principles of the uncertainty transformation. In the following, the theoretical background and problem formulation of this study are presented in Section 2. Section 3 reports the analysis and discussions for different application scenarios. This is followed by some recommendations for practical microwave measurements. Finally, conclusion of this study is given in Section 4.

2. THEORETICAL BACKGROUND AND PROBLEM FORMULATION

In this paper, a complex-valued quantity S is represented by its real and imaginary components R and I as,

$$S = R + jI \tag{1}$$

It is noted that the measurand S is often assumed to be bivariate normal distributed on the origin of a complex plane for repeated measurements [10, 12]. Works in [10] strongly recommended the measurement uncertainty of a complex-valued quantity should be analyzed first in terms of its real and imaginary components, and then transformed into the desired polar representation for the magnitude and phase.

Following the guidelines in [5], the standard uncertainties $u(R)$ and $u(I)$ for the real and imaginary components R and I can be estimated accordingly. The covariance matrix $V(S)$ for S can therefore be obtained as

$$V(S) = \begin{bmatrix} u^2(R) & ru(R)u(I) \\ ru(R)u(I) & u^2(I) \end{bmatrix} \tag{2}$$

where r is the sample correlation coefficient between R and I.

In this study, for the non-linear transformation from rectangular coordinate to polar coordinate, Jacobian matrix is used. For the magnitude $|S|$ with

$$|S| = \sqrt{R^2 + I^2}. \tag{3}$$

We can derive the followings,

$$\frac{\partial |S|}{\partial R} = \frac{R}{\sqrt{R^2 + I^2}}, \quad \frac{\partial |S|}{\partial I} = \frac{I}{\sqrt{R^2 + I^2}}. \tag{4}$$

Its Jacobian matrix $J_{|S|}$ for the coordinate transformation is

$$J_{|S|} = \begin{bmatrix} \dfrac{\partial |S|}{\partial R} & \dfrac{\partial |S|}{\partial I} \end{bmatrix}. \tag{5}$$

Following the *law of propagation of uncertainty* in matrix form, the covariance matrix $V(|S|)$ for the magnitude $|S|$ can be obtained through [10, 13, 14],

$$V(|S|) = J_{|S|}V(S)J_{|S|}^T. \tag{6}$$

That is,

$$V(|S|) = \frac{u^2(R)R^2 + u^2(I)I^2}{R^2 + I^2} + r\frac{2u(R)u(I)RI}{R^2 + I^2}. \tag{7}$$

Similarly, the covariance matrix $V(\phi)$ for the phase ϕ can be obtained as,

$$\phi = \tan^{-1}\left(\frac{I}{R}\right), \tag{8}$$

$$V(\phi) = \frac{u^2(R)I^2 + u^2(I)R^2}{(R^2 + I^2)^2} - r\frac{2u(R)u(I)RI}{(R^2 + I^2)^2}. \tag{9}$$

From (7) and (9), it is observed that the covariance matrices $V(|S|)$ and $V(\phi)$ rely on the sample correlation coefficient r between R and I. However, the coefficient r is inherently unreliable due to the small sample size in practical measurements [10]. Therefore, detailed investigations of the influence from the variation of correlation coefficient r on the evaluated measurement uncertainties in polar coordinate are important and then carried out in this study.

3. CASE STUDIES AND ANALYSIS

3.1. For the Case: $u(R) = u(I) = u$, and $r = 0$

This is the simplest case of uncertainty evaluations for a complex-valued quantity. When $u(R) = u(I) = u$ and $r = 0$, $V(|S|)$ and $V(\phi)$ in (7) and (9) can be simplified as,

$$V(|S|) = u^2, \quad V(\phi) = \frac{u^2}{R^2 + I^2}. \tag{10}$$

The standard uncertainty of the magnitude $|S|$ and the phase ϕ can be then obtained as,

$$u(|S|) = u, \quad u(\phi) = \frac{u}{|S|}. \tag{11}$$

It is noted the phase uncertainty $u(\phi)$ is in the unit of radian. The simplified forms in (11) are consistent with those reported in [11]. Study in [11] also reveals that the phase uncertainty $u(\phi)$ for a complex-valued quantity is open to different suggestions such as

$u(\phi) = \tan^{-1}(u/|S|)$ in [13] and $u(\phi) = \sin^{-1}(u/|S|)$ in [15]. Both the equations in [13, 15] are actually derived from slightly different geometrical considerations. When $u/|S|$ is small (e.g., the reflection coefficient of a highly reflecting RF component which has a small uncertainty u but with a magnitude $|S|$ very close to unity), they are virtually equal.

Before embarking on the physical interpretations of the derived standard uncertainties in polar coordinate, geometric representation for the uncertainty of a complex-valued quantity $(S = R + jI)$ is investigated as a region in the complex plane around its best estimate $(\bar{S} = \bar{R} + j\bar{I})$. To predict the uncertainty region with a 95% level of confidence from repeated measurements, a circle centred at $(\bar{R}, \bar{I})$ with its radius of U can provide an uncertainty region with the desired coverage probability where

$$U = k_{2d}\bar{u}. \qquad (12)$$

$\bar{R}, \bar{I}$, and $\bar{u}$ are the estimated mean values of the real and imaginary components and their standard uncertainty. k_{2d} is the two-dimensional coverage factor for the 95% coverage probability and is around 2.45 [10, 11].

Numerical simulations are then performed in this study using the R-programming language which is a free software designed for statistical computing [16]. Bivariate normal distribution is used to simulate a complex-valued measurand S from an experiment with $R = 0.02666$, $I = -0.05508$, $u = 0.01572$, and $r = 0$. These assigned
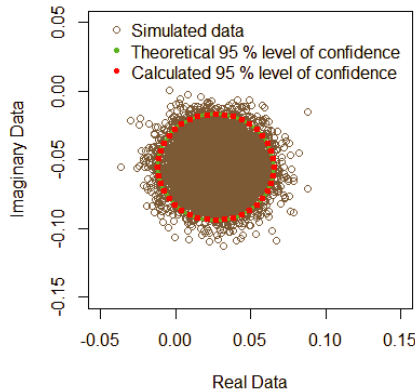
Figure 1. Simulated 10000 repeated measurements with both theoretical and calculated circular uncertainty regions (95% level of confidence) with $R = 0.02666$, $I = -0.05508$, $u = 0.01572$, and $r = 0$.

values are from the realistic measurements during calibrations in NMC. Simulated results with 10000 repeated measurements are plotted in Fig. 1 together with both the theoretical and calculated uncertainty regions at 95% level of confidence.

From Fig. 1, it can be found that the calculated uncertainty region matches well with the theoretical one. That is for practical measurements, a circle centred at $(\bar{R}, \bar{I})$ with a radius of $U = k_{2d}\bar{u}$ can well estimate the uncertainty region with a 95% coverage probability if the standard uncertainties for both the real and imaginary components approach the same and there is no correlation ($r = 0$) between R and I.

A geometry representation of the circular uncertainty region is shown in Fig. 2 for understanding the principles of uncertainty coordinate transformation. From Fig. 2, the uncertainty estimations for the magnitude $|S|$ and the phase ϕ when $u(R) = u(I) = u$ and $r = 0$ using (11) can be easily interpreted. For the uncertainty of magnitude $|S|$, $[|\bar{S}| - k_{2d}\bar{u}, |\bar{S}| + k_{2d}\bar{u}]$ can provide an uncertainty region with a 95% level of confidence. For the uncertainty of phase ϕ, there is little practical difference among the above-mentioned three methodologies if $\bar{u}/|\bar{S}| \ll 1$, and either of them can be used to estimate the phase uncertainty properly. However in practical situations, uncertainties of the real and imaginary components are generally not equal and even correlated. Therefore, further investigations of more complex cases are required and then performed in the followings. Moreover, it is noted that when the uncertainty region lies close to the origin of the complex plane (i.e., centre $(\bar{R}, \bar{I})$ is near to the origin $(0, 0)$), the uncertainty region is distorted and the coverage probability is difficult to predict as described in [11].

3.2. For the Case: $u(R) \neq u(I)$, and $r = 0$

This is the case when there is no correlation (i.e., $r = 0$) between the real and imaginary components, and their standard uncertainties $u(R)$ and $u(I)$ are not equal. Same as in Section 3.1, the standard uncertainties of the magnitude $|S|$ and the phase ϕ can be obtained from (7) and (9) as,

$$u(|S|) = \frac{\sqrt{u^2(R)R^2 + u^2(I)I^2}}{|S|} \tag{13}$$

$$u(\phi) = \frac{\sqrt{u^2(R)I^2 + u^2(I)R^2}}{|S|^2}. \tag{14}$$

Different from the circular uncertainty region described in Section 3.1, an elliptical uncertainty region is produced when
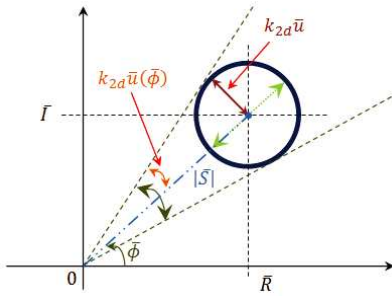
Figure 2. Geometry of circular uncertainty region for coordinate transformation.
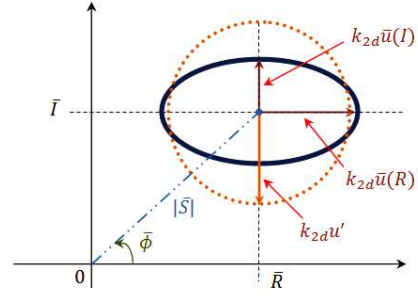
Figure 3. Geometry of uncertainty regions for a circular one that is approximate to an elliptical one.

$u(R) \neq u(I)$. It is therefore not easy to correlate the derived standard uncertainties in (13) and (14) to the geometry uncertainty representation.

Hence, an alternative way is then used in this study to investigate the reliabilities of (13) and (14). The evaluated uncertainties are compared to some reference values with known coverage probability. To utilize the observations in Section 3.1, a circular uncertainty region with a standard uncertainty u' which is approximate to the elliptical uncertainty region as shown in Fig. 3 is used as a reference. The standard uncertainty u' could be equal to $u_{\max}$ or u_{rms}, where $u_{\max}$ is the maximum standard uncertainty of $u(R)$ and $u(I)$ and defined as

$$u_{\max} = \max(u(R),\, u(I)). \tag{15}$$

u_{rms} is the rms (root-mean-square) standard uncertainty of $u(R)$ and $u(I)$ which is described in [11] as,

$$u_{rms} = \sqrt{\frac{u^2(R) + u^2(I)}{2}}. \tag{16}$$

Simulations for 10000 repetitions of measurements using the bivariate normal distribution function with $R = 0.02666$, $I = -0.05508$, $u(R) = 0.02572$, $u(I) = 0.01572$, and $r = 0$, are performed. The estimated uncertainties and the coverage probability using the different methods are summarized in Table 1.

From Table 1, it is found that the estimated uncertainties for $u' = u_{\max}$ or u_{rms} are larger than the values using our methods in (13) and (14). This is because partial circular uncertainty regions are empty when $u' = u_{\max}$ or u_{rms} as shown in Fig. 4, which makes

the uncertainty overestimated in polar coordinate. Moreover, it is also found that the uncertainty evaluated by the *max* circular region ($u' = u_{\max}$) is the maximum of three with a coverage probability 98% (larger than 95% requirement). That is, its evaluated uncertainty could be treated as an upper boundary with high confidence.

To further investigate our method in this study, we compare the estimated magnitude uncertainty using (13) to the value by applying statistics to the magnitude $|S|$ directly (The method is not recommended for a complex-valued quantity as the calculation of the uncertainty in this way underestimates the "true" underlying uncertainty [10]). The direct evaluation of the magnitude uncertainty leads to a value of 0.0176, while our result of 0.0181 in Table 1 which is larger than the direct evaluation looks reasonable.

Table 1. Results of the estimated standard uncertainties of the magnitude $|S|$ and the phase ϕ and their coverage probability $P\%$.

Method	$u(|S|)$	$u(\phi)$	$P\%$
$u' = u_{\max}$	∼0.0256	∼1.021	∼98.0
$u' = u_{rms}$	∼0.0213	∼0.849	∼94.3
Ours u_{ours}	∼0.0181	∼0.392	-
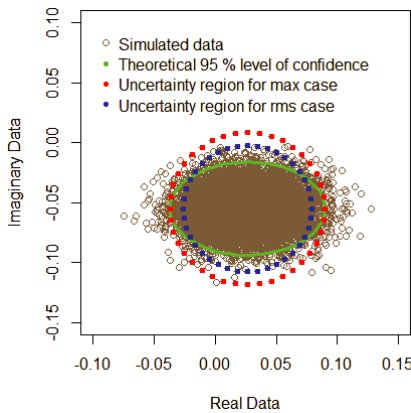
Figure 4. Simulated 10000 repeated measurements with the different uncertainty regions ($R = 0.02666$, $I = -0.05508$, $u(R) = 0.02572$, $u(I) = 0.01572$, and $r = 0$).
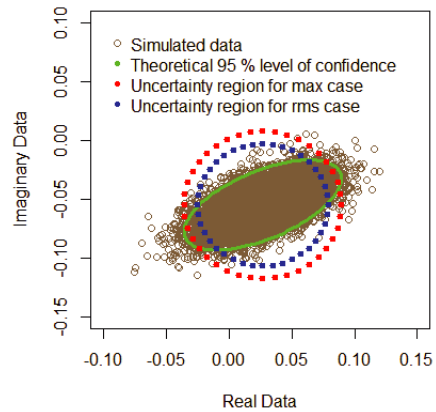
Figure 5. Simulated 10000 repeated measurements with the different uncertainty regions ($R = 0.02666$, $I = -0.05508$, $u(R) = 0.02572$, $u(I) = 0.01572$, and $r = 0.6$).

3.3. For the Case: $u(R) \neq u(I)$, and $r \neq 0$

This is the general case for the coordinate transformation with a bounded quantity $r \in [-1, 1]$. The eigenvalues of the covariance matrix (2) do not hold a simple relationship to the standard uncertainties $u(R)$ and $u(I)$ of the real and imaginary components. For most of the practical measurements, the estimated r is inherently unreliable due to the relatively small sample size. Therefore, it is difficult to realize the coordinate transformations with (7) and (9), where linear relationships between $V(|S|)$ (or $V(\phi)$) and r are observed.

Hence, $u(|S|)$ and $u(\phi)$ at the boundary conditions ($r = \pm 1$) as shown in (17) to (20) can be considered to determine the uncertainty ranges for the magnitude $|S|$ and the phase ϕ.

$$u(|S|)_{r=1} = \frac{|u(R)R + u(I)I|}{|S|} \tag{17}$$

$$u(|S|)_{r=-1} = \frac{|u(R)R - u(I)I|}{|S|} \tag{18}$$

$$u(\phi)_{r=1} = \frac{|u(R)I - u(I)R|}{|S|^2} \tag{19}$$

$$u(\phi)_{r=-1} = \frac{|u(R)I + u(I)R|}{|S|^2} \tag{20}$$

From our study in [3], it is observed that when $r = \pm 1$, upper and lower boundaries for $u(|S|)$ and $u(\phi)$ are formed. Therefore, to provide a confident uncertainty region, $u(|S|)$ and $u(\phi)$ can be evaluated through,

$$u(|S|) = \max(u(|S|)_{r=1}, u(|S|)_{r=-1}) \tag{21}$$
$$u(\phi) = \max(u(\phi)_{r=1}, u(\phi)_{r=-1}). \tag{22}$$

Simulations for 10000 repetitions of measurements using the bivariate normal distribution function with $R = 0.02666$, $I = -0.05508$, $u(R) = 0.02572$, and $u(I) = 0.01572$, are performed by varying r in the range of $[-1, 1]$ at a step of 0.1. An example of the simulated results at $r = 0.6$ is shown in Fig. 5 for reference. Same as in Section 3.2, comparisons of the estimated uncertainty results using (21) and (22) are performed against the evaluated results from the circular uncertainty regions with the standard uncertainty $u' = u_{max}$ or u_{rms} in (15) and (16), and also the results by the direct evaluation of the magnitude $|S|$ although it is not recommended. The estimated results are summarized and plotted in Fig. 6 to Fig. 8 respectively.

The evaluated standard uncertainties for the magnitude $|S|$ using the above-mentioned different methods are shown in Fig. 6. From

Fig. 6, it is found that the results by the direct evaluation of magnitude $|S|$ are decreasing when the sample correlation coefficient r increases, while the uncertainties estimated by other three methods are almost kept constant regardless of r. As the sample correlation coefficient r is inherently unreliable for practical measurements due to the relatively small sample size, the directly evaluated uncertainty for the magnitude $|S|$ is therefore less reliable as it is the correlation coefficient r
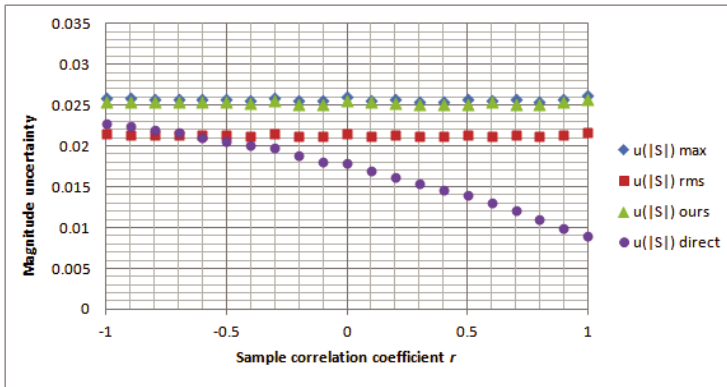
Figure 6. Evaluated uncertainty for the magnitude $|S|$ using different methods when $R = 0.02666$, $I = -0.05508$, $u(R) = 0.02572$, $u(I) = 0.01572$, and $r \in [-1, 1]$.
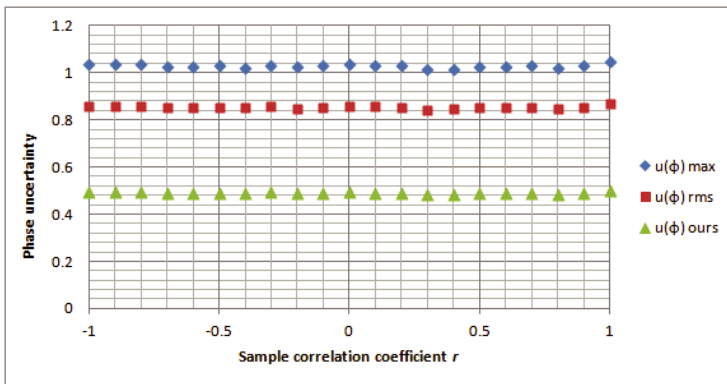
Figure 7. Evaluated uncertainty for the phase ϕ using different methods when $R = 0.02666$, $I = -0.05508$, $u(R) = 0.02572$, $u(I) = 0.01572$, and $r \in [-1, 1]$.
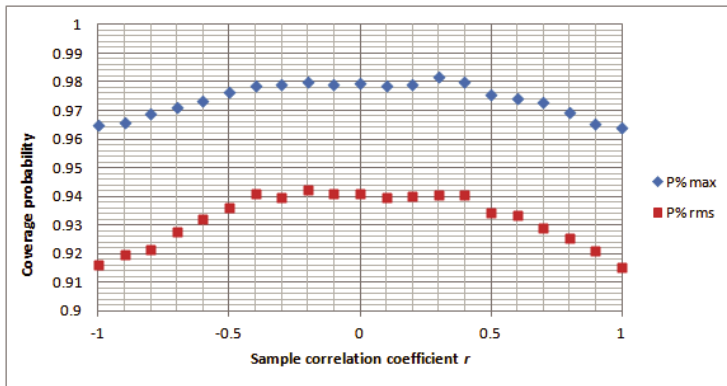
Figure 8. Evaluated coverage probability using a circular uncertainty region with the standard uncertainty $u' = u_{\max}$ or u_{rms} when $R = 0.02666$, $I = -0.05508$, $u(R) = 0.02572$, $u(I) = 0.01572$, and $r \in [-1, 1]$.

dependent.

Further investigations are then performed among the other three methods (uncertainty evaluation using the *max* circular region (15), uncertainty evaluation using the *rms* circular region (16), and our method using (21) and (22). The evaluated uncertainties for phase ϕ using the three methods are shown in Fig. 7. Together with Fig. 6, it is found that, the uncertainty evaluation using the *max* circular region can be treated as an upper boundary for both the magnitude $|S|$ and the phase ϕ, especially its coverage probability is at least 96% regardless of r as observed in Fig. 8.

However, it is hard to reach a conclusion on the performances of uncertainty evaluations using the *rms* circular region and our method using (21) and (22). For the evaluation using the *rms* circular region, it should be noted that when the real and imaginary components are highly correlated, its coverage probability will degrease gradually to around 91.5% as shown in Fig. 8. It is also interesting to note that, the coverage probability for the uncertainty evaluation using the *rms* circular region is almost constant and around 94% when $|r| < 0.4$. Moreover, our method is more sensitive to the values of the real and imaginary components as observed in (17) to (20). Therefore, proper selection of the above methods for uncertainty evaluation is required and important in the practical microwave measurements. If there is limited information about the measurand, its uncertainty is recommended to be evaluated using the *max* circular region.

4. CONCLUSIONS

This paper reports an evaluation of measurement uncertainty for complex-valued quantities in microwave applications. The *law of propagation of uncertainty* in matrix form has been used to derive the general expressions of covariance matrix for the magnitude and phase uncertainties in polar coordinate.

Through the investigations of different application scenarios with numerical simulations, we found that the uncertainty evaluation using the *max* circular region can be treated as an upper boundary for both the magnitude and phase uncertainties regardless of the correlation between the real and imaginary components. Moreover, for the evaluations of measurement uncertainty in practical microwave measurements, proper method should be selected basing on the known property of the complex-valued quantities.

REFERENCES

1. Shan, Y., L. Oberto, Y. S. Meng, H. Neo, L. Brunetti, and M. Sellone, "Scattering parameter measurement comparison between NMC and INRIM on vector network analyzer using WR15 and WR10 connectors," *CPEM 2012 Digest*, 96–97, Washington DC, USA, 2012.

2. Meng, Y. S., Y. Shan, and H. Neo, "Development of a waveguide microwave power sensor calibration system at NMC," *APEMC 2012 Proceedings*, 745–748, Singapore, 2012.

3. Meng, Y. S., Y. Shan, and H. Neo, "Evaluation of complex measurement uncertainty in polar coordinate for equivalent source reflection coefficient," *CPEM 2012 Digest*, 116–117, Washington DC, USA, 2012.

4. Shan, Y. and X. Cui, "RF and microwave power sensor calibration by direct comparison transfer," *Modern Metrology Concerns*, Chapter 7, 175–200, ISBN: 978-953-51-0584-8, 2012.

5. BIPM, IEC, IFCC, ILAC, ISO, IUPAC, IUPAP, OIML, "Evaluation of measurement data — Guide to the expression of uncertainty in measurement," JCGM 100:2008 (GUM 1995 with Minor Corrections), BIPM Joint Committee for Guides in Metrology, 2008.

6. Wang, Z., W. Che, and L. Zhou, "Uncertainty analysis of the rational function model used in the complex permittivity measurement of biological tissues using PMCT probes within a

wide microwave frequency band," *Progress In Electromagnetics Research*, Vol. 90, 137–150, 2009.

7. Azpurua, M. A., C. Tremola, and E. Paez, "Comparison of the gum and monte carlo methods for the uncertainty estimation in electromagnetic compatibility testing," *Progress In Electromagnetics Research B*, Vol. 34, 125–144, 2011.

8. Haarscher, A., P. De Doncker, and D. Lautru, "Uncertainty propagation and sensitivity analysis in ray-tracing simulations," *Progress In Electromagnetics Research M*, Vol. 21, 149–161, 2011.

9. Paez, E., M. A. Azpurua, C. Tremola, and R. C. Callarotti, "Uncertainty estimation in complex permittivity measurements by shielded dielectric resonator technique using the monte carlo method," *Progress In Electromagnetics Research B*, Vol. 41, 101–119, 2012.

10. Ridler, N. M., and M. J. Salter, "An approach to the treatment of uncertainty in complex S-parameter measurements," *Metrologia*, Vol. 39, No. 3, 295–302, 2002.

11. Hall, B. D., "Notes on complex measurement uncertainty — Part 1," Tech. Rep. 2483, Industrial Research Ltd., New Zealand, 2010.

12. Hall, B. D., "Calculating measurement uncertainty for complex-valued quantities," *Measurement Science and Technology*, Vol. 14, No. 3, 368–375, 2003.

13. Hall, B. D., "Some considerations related to the evaluation of measurement uncertainty for complex-valued quantities in radio frequency measurements," *Metrologia*, Vol. 44, No. 6, L62–L67, 2007.

14. Hall, B. D., "On the propagation of uncertainty in complex-valued quantities," *Metrologia*, Vol. 41, No. 3, 173–177, 2004.

15. Ridler, N. M., and J. C. Medley, "An uncertainty budget for VHF and UHF reflectometers," NPL Rep. DES 120, National Physical Laboratory, UK, 1992.

16. R Development Core Team, "R: A language and environment for statistical computing," R Foundation for Statistical Computing, Vienna, 2009, http://www.r-project.org/.